Near-infrared electro-optic modulator based on plasmonic graphene

Susbhan Das,[1] Alessandro Salandrino,[1] Judy Z. Wu,[2] and Rongqing Hui[1,*]

[1]*Department of Electrical Engineering and Computer Science, the University of Kansas, Lawrence, Kansas 66045, USA*

[2]*Department of Physics and Astronomy, the University of Kansas, Lawrence, Kansas 66045, USA*

*Corresponding author: rhui@ku.edu

We propose a novel scheme for an electro-optic modulator based on plasmonically enhanced graphene. As opposed to previously reported designs where the switchable absorption of graphene itself was employed for modulation, here a graphene monolayer is used to actively tune the plasmonic resonance condition through the modification of interaction between optical field and an indium tin oxide (ITO) plasmonic structure. Strong plasmonic resonance in the near infrared wavelength region can be supported by accurate design of ITO structures, and tuning the graphene chemical potential through electrical gating switches on and off the ITO plasmonic resonance. This provides much increased electro-absorption efficiency as compared to systems relying only on the tunable absorption of the graphene.   © 2015 Optical Society of America

OCIS codes: (130.3120) Integrated optics devices; (250.0250) Optoelectronics; (130.4815) Optical switching devices; (060.2370) Fiber optics sensors; (130.4110) Modulators.

http://dx.doi.org/10.1364/OL.40.001516

Due to the exceptional optical and electronic properties, graphene has attracted a great deal of attention in the scientific and engineering communities [1]. The two-dimensional (2D) atomic structure of graphene leads to a low density of states for electrons and holes, making the chemical potential particularly susceptible to the density of carriers. The large shift in the chemical potential that can be achieved by applying a gate electric field across the graphene layer produces an extra charge accumulation in the energy bands and enhances both inter-band and intra-band electron transitions, allowing for efficient tuning of graphene's electric and optical properties. Such mechanisms have been successfully exploited for many practical applications, such as field effect transistors [2,3], photodetectors [4,5], and electro-optic modulators [6,7].

The graphene-based electro-optic modulator relies on the gate voltage-dependent optical absorption of graphene [6,7]. Although the absorption coefficient of graphene is extremely large compared with other materials commonly used in the near infrared (NIR) spectrum (3 orders of magnitude higher than that of germanium at 1.5 μm, and 4 orders of magnitude higher than that of silicon at 1 μm), the total absorption of a monolayer graphene is only about 2.3% for vertically incident light, simply because of the atomic thickness. Planar waveguide structures have been implemented to increase the interaction length between the guided-mode optical field and the graphene [4,5]. An electro-absorption optical modulator with 10-dB extinction ratio was achieved with a 100-μm-long silicon waveguide embedded with a monolayer graphene [6]. Because the mode field diameter of a silicon optical waveguide is approximately 4 orders of magnitude larger than the thickness of a monolayer graphene, the interaction between the optical field and the graphene is intrinsically weak. As a consequence, the modulator has to have long enough waveguide to achieve the required electro-optic tunability and the signal extinction ratio, which would result in relatively large capacitance, slow modulation speed, and large electrical

power consumption. Thus, enhancing the interaction of optical signals with graphene is critically important to realize practical electro-optic devices that rely on the tunability of graphene.

We propose here a novel hybrid photonic–plasmonic platform for the realization of a graphene-based optical modulator operating at telecommunication wavelengths. Plasmonic structures represent an interesting avenue for the enhancement of light–matter interaction in graphene monolayers, mediated by the strong local optical field associated with surface plasmonic resonances [8]. In fact, plasmonic excitations in micro/nano-structured graphene have been explored in far-infrared (FIR) and THz spectral regions [9–11]. In the previously reported graphene-based NIR electro-absorption modulators, modulation is based on the tunable absorption of graphene, while in the present scheme, the graphene provides a mechanism of tuning on and off the resonant absorption of a plasmonic waveguide. As conventional noble metals such as Au and Ag have their plasma frequency in the visible or ultraviolet (UV) wavelengths, we have considered photonic waveguides loaded with indium tin oxide (ITO) nanostructures placed in close proximity of the graphene layer to maximize the sensitivity of the plasmonic resonance to the dielectric properties of graphene in the NIR region. In exploiting this mechanism, we have designed an ultra-compact graphene-based plasmonic electro-absorption modulator that is able to achieve an order of magnitude reduction in the required waveguide length as compared to a graphene-based all-dielectric modulator.

The configuration of the proposed electro-absorption modulator is schematically shown in Fig. 1, which is based on a silicon ridge waveguide fabricated on a silicon-on-insulator (SOI) wafer. A monolayer graphene sandwiched in the middle of the waveguide provides the mechanism of electro-optic interaction through the modulation of its chemical potential. A 10-nm-thick dielectric layer of HfO_2 is placed underneath the graphene to electrically isolate the top and the bottom parts of the silicon waveguide. The width and height of the
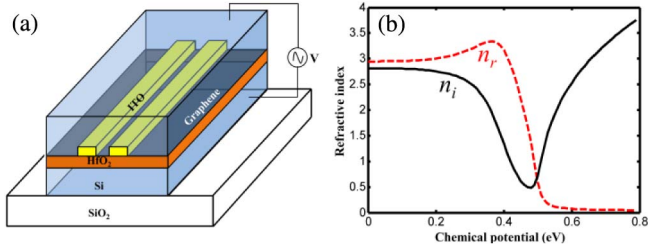
Fig. 1.   (a) Schematic diagram of the hybrid plasmonic waveguide. (b) In-plane refractive index of graphene as the function of chemical potential at 1550-nm wavelength.

waveguide are 420 and 300 nm, respectively. To enhance the interaction between optical field and the graphene, a number of ITO bars are placed on top of the graphene layer to introduce the plasmonic effect. To simplify the analysis, the minimum separation between adjacent ITO bars was set as 10 nm, which is longer than the decay length of plasmonic near-field, and the coupling of plasmonic modes between ITO bars was negligible. In this configuration, the resonance condition of the plasmonic mode is susceptive to the dielectric constant of the surrounding materials including the graphene.

The complex conductivity of monolayer graphene can be calculated using the well-known Kubo's formula [12], as shown in Eq. (1), which is the combination of the inter-band and intra-band absorptions represented by the 1st and the 2nd term, respectively. ω is the optical frequency, e is the electron charge, $\hbar = h/2\pi$ is the reduced Planck's constant, $f_d(\varepsilon) = 1/(e^{(\varepsilon-\mu_c)/k_BT} + 1)$ is the Fermi–Dirac distribution function, ε is the energy, k_B is the Boltzmann's constant, μ_c is the chemical potential, T is the absolute temperature, and Γ is the scattering parameter. $T = 300$ K and $\Gamma = 5$ meV [13] was used in the calculation. The conductivity predicted by Eq. (1) can be converted into an in-plane complex refractive index: $n_g = \sqrt{1 - j\sigma/(\omega\varepsilon_0\delta_g)}$, where ε_0 is the free space permittivity, and $\delta_g = 0.34$ nm is the thickness of monolayer graphene. $n_g = 1$ for the out-of-plane index of graphene. At 1550-nm optical communications wavelength, the in-plane refractive index of graphene as the function of chemical potential is shown in Fig. 1(b), where the imaginary part n_i is primarily responsible for optical absorption.

Electro-absorption modulator based on monolayer graphene embedded in silicon ridge waveguide has been reported previously, with a maximum absorption efficiency of 0.1 dB/μm determined by the graphene in the waveguide [6], which was later increased to 0.16 dB/μm by using two separate layers of graphene in the waveguide [7]. The absorption efficiency of these modulators was primarily limited by the low interaction between the propagating mode of the waveguide and the atomic-thin graphene layer. In order to achieve a 20-dB extinction ratio typically required in telecommunications, the waveguide length has to be longer than 100 μm. The device capacitance, C_p, linearly proportional to the waveguide length, is a major limiting factor for practical applications, which causes slow modulation speed and high power consumption.

Surface plasmon resonances can be effective to confine the optical field far below the diffraction limit, and therefore to enhance the interaction between the optical field and the graphene placed in the plasmonic near-field region. The strength of plasmonic resonance is proportional to $1/(\varepsilon_m + M\varepsilon_b)$ where ε_m and ε_b are permittivities of the metal and the surrounding dielectric materials, respectively. M is a structural-dependent factor that varies with the geometry but is typically of the order of 1. Therefore, the conditions for plasmonic resonance can be met when the metallic permittivity is nearly opposite to the permittivity of the surrounding medium. Although noble metals, such as Au and Ag, are commonly used to create surface plasmonic effect, the negative values of their permittivities are very large, and their plasmonic resonances are typically in the visible wavelengths [14–16]. In comparison, transparent conducting oxide (TCO) such as ITO has a much smaller permittivity (also negative), allowing for the plasmonic resonance to be in the NIR wavelength region, and the permittivity value can be modified by the change of carrier density through

$$\sigma(\omega, \mu_c, \Gamma, T)$$
$$= \frac{je^2(\omega - j2\Gamma)}{\pi\hbar^2}\left\{\frac{1}{(\omega - j2\Gamma)^2}\int_0^\infty \varepsilon\left[\frac{\partial f_d(\varepsilon)}{\partial\varepsilon} - \frac{\partial f_d(-\varepsilon)}{\partial\varepsilon}\right]d\varepsilon\right.$$
$$\left. - \int_0^\infty \left[\frac{f_d(\varepsilon) - f_d(-\varepsilon)}{(\omega - j2\Gamma)^2 - 4\left(\frac{\varepsilon}{\hbar}\right)^2}\right]d\varepsilon\right\} \quad (1)$$

doping [17,18]. This permits precise tuning of resonance wavelength suitable for different dielectric constants of the surrounding materials. Therefore, the plasmonic effect introduced by the TCO bars shown in Fig. 1 can help concentrate the NIR optical field into the monolayer graphene, and the efficiency of electro-absorption can be significantly enhanced.

Figure 2 illustrates the effects of one ITO rod on the waveguide dispersion. The blue curve represents the effective index of the waveguide without the embedded ITO rod. The red curve represents the effective index of the waveguide when one embedded ITO rod rests on the HfO$_2$ layer. The effect of the ITO structure is to modify the effective index of the fundamental mode of the
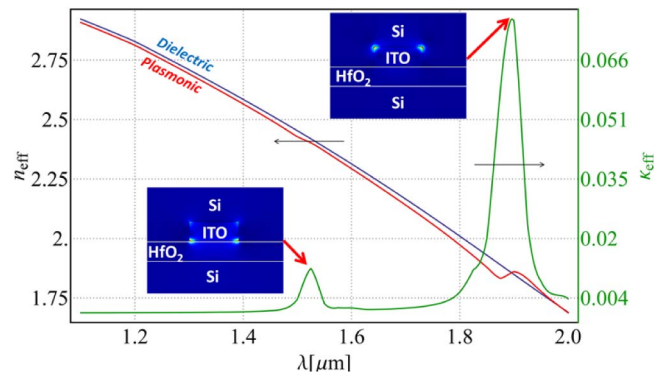
Fig. 2.   Waveguide dispersion curves for effective index and absorption coefficient with and without ITO bars. The insets show the norm of the electric field distribution around the ITO structure.

waveguide by providing a source of dielectric polarization. Notice that the effective index of the mode in the ITO loaded waveguide is almost uniformly lower than the index of the unperturbed dielectric waveguide, except for the spectral region near the second resonant peak around 1875 nm. In any case, the effective index of the mode never exceeds the index of the Si background medium. This is an indication that the ITO structure is operating on a localized transverse plasmonic resonance, without supporting a guided plasmon polariton along the waveguide. This interpretation is consistent with the field distributions shown in the insets of Fig. 2. For the telecommunication applications, we are primarily interested in the spectral region near 1550 nm, where the electric field of the surface plasmon is localized at the ITO-HfO$_2$ interface, consistent with the fact that the permittivity of the two media are nearly opposite. A strong plasmonic resonance also appears around 1875 nm but with the electric field mainly concentrated at the ITO-Si interface and the overlap between the resonant mode field pattern and the graphene layer is weak, thus the resonance condition is less susceptible to the conductivity changes in graphene. Notice that the bandwidth of the resonance near 1550-nm wavelength is wider than 30 nm, making it suitable for optical communication applications.

It is important to point out that the fundamental mode field distribution is not significantly altered by the ITO rod, except for the enhanced field in proximity of the plasmonic structure. As a consequence of these mode-matching considerations, the reflection at the junction with a simple Si input guide of similar cross-section are expected to be negligible.

Figure 3 shows the comparison of electric field intensity on the graphene layer with and without the ITO bars. The field pattern shown in the inset of Fig. 3(b) refers the 1550-nm resonance in the presence of unbiased graphene (high absorption state). The presence of graphene modifies the plasmonic field distribution reducing the intensity of the hot-spots at the corners of the ITO-HfO$_2$ interface. Nevertheless, it is evident that optical field concentration on graphene is increased by approximately 2 orders of magnitude underneath the ITO bars because of the plasmonic effect. The simulations were performed with COMSOL multiphysics software package, and the following parameters were used in the simulation: $\varepsilon_d = 4$ is the permittivity of HfO$_2$, and $\varepsilon_m = -3.99 + j0.13$ is the permittivity of ITO at 1550-nm wavelength, corresponding to a doping density of 1.37×10^{27} m^{-3} [17]. The permittivity of silicon is $\varepsilon_{si} = 12.3$, which is used as the dielectric medium to form the waveguide core. Because
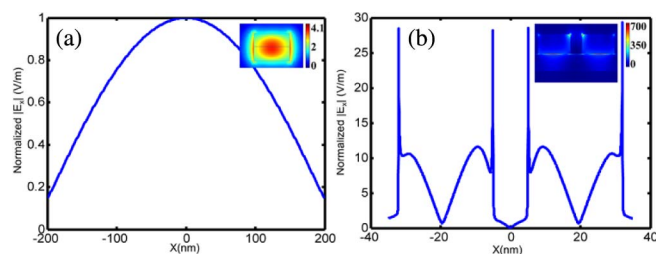
the dielectric materials surrounding the ITO bars, including HfO$_2$, silicon, and graphene, have different permittivity values, their combined effect determines the plasmonic resonance wavelength. The complex dielectric constant of graphene is a function of its chemical potential μ_c, and optical absorption can be turned from on to off when μ_c is switched from 0 to approximately 0.5 eV as shown in Fig. 1(b). This not only allows the electric control of optical absorption but also provides an effective mechanism of switching on and off the plasmonic resonance when ITO bars are used.

To maximize the differential absorption of the NIR optical signal introduced by electrical gating, the cross-section geometry of ITO bars can be varied for optimization. Figure 4 shows the calculated optical absorption per unit length along the waveguide by varying the width [Fig. 4(a)] and height [Fig. 4(b)] of the ITO bar cross-section. This was calculated with a single ITO bar placed on graphene layer in the middle of the waveguide. The absorption corresponding to 0 and 0.5 eV of graphene chemical potential shown in Fig. 4 represent the maximum and the minimum loss values, and their difference indicates the extinction (on/off) ratio the modulator can provide. Figure 4 shows that the extinction ratio can be maximized by optimizing the geometry of the ITO bar cross-section, which indicates that tuning of plasmonic resonance condition through graphene chemical potential is the dominant mechanism in this plasmonic-graphene guided mode structure. This is fundamentally different from the graphene-based modulators previously reported [6,7], where electro-optic absorption of the graphene itself was the dominant mechanism, and thus the value of absorption per unit waveguide length was intrinsically low. In the example shown in Fig. 4, the optimum width and height of the ITO bar are in the vicinity of 27 and 12 nm, respectively.

As the width of the graphene layer in the silicon waveguide is 400 nm, multiple parallel ITO bars can be used to further enhance the efficiency of controllable absorption. Figure 5 shows the calculated unit-length absorption of the plasmon mode as the function of the graphene chemical potential for different numbers of ITO bars separated by 10 nm between each other. By increasing the number of ITO bars, the maximum differential absorption increases almost linearly because the 10-nm separation between them is much longer than the spreading of the plasmonic near field, and thus interaction between plasmon modes of different ITO bars is negligible.

Fig. 3.   Normalized electrical field $|E_x|$ distributions at 1550 nm on the graphene layer of a graphene-embedded SOI ridge waveguide without (a) and with (b) two ITO bars on the graphene.
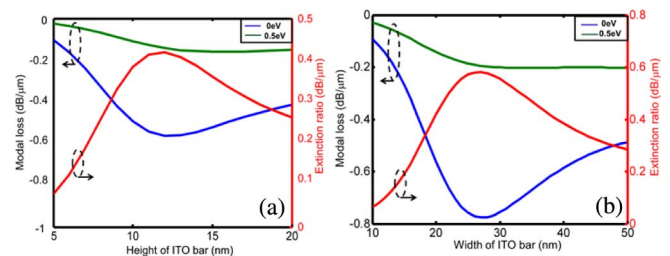
Fig. 4.   (a) Modal loss and extinction ratio for different height of the ITO bar with a fixed 20-nm width. (b) Modal loss and extinction ratio for different width of the ITO bar with a fixed 12-nm height.
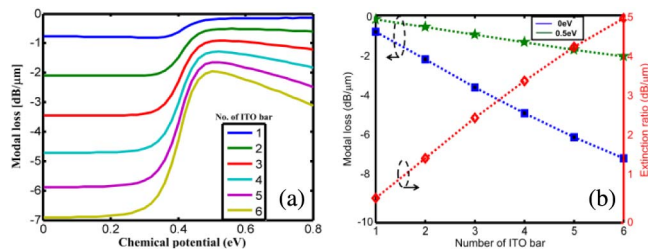
Fig. 5.   (a) Modal loss per μm as the function of graphene chemical potential for the waveguide with different number of ITO bars, and (b) modal loss at 0 and 0.5-eV graphene chemical potential for different number of ITO bars, and the corresponding extinction ratio.

Although up to 10 ITO bars can be accommodated over the 400-nm wide graphene layer, a large number of ITO bars not only increases the extinction ratio, but also increases the minimum loss of the modulator, so that a trade-off has to be made for practical applications. For example, for a modulator using six ITO bars, the extinction ratio reaches to approximately 5 dB/μm, which is more than an order of magnitude higher than that without the plasmonic effect. According to Fig. 5(b), the configuration with six ITO bars also suffers from an insertion loss of about 1.7 dB/μm, which is a disadvantage common for optical circuits involving plasmonic effect. A trade-off has to be made between the extinction ratio and the insertion loss when choosing the waveguide length. Nevertheless, the combination of plasmonic elements with a graphene layer allows significant reduction of the waveguide length and the size of the electrode, which is essential to reduce the intrinsic capacitance of the device for high-speed operation with low power consumption.

Practically, the deposition of materials on graphene is difficult with many conventional physical or chemical vapor depositions as energetic particles and reactive chemicals from the deposition sources cause damages on graphene. This problem may be solved by evaporating a thin protecting interfacial layer such as Al film on graphene and converting it to insulating AlOx upon exposure to oxygen before ITO and Si layers growth atop using atomic layer deposition. [19,20]

In conclusion, we have proposed a highly efficient electro-optic modulation mechanism based on plasmonic graphene for applications in NIR optical communications wavelength. ITO is used to produce plasmon resonance at the NIR wavelength, and the interaction between optical field and monolayer graphene is significantly enhanced by the plasmonic effect. Tuning of graphene chemical potential through electrical gating switches on and off the ITO plasmonic resonance, providing much increased electro-optic efficiency compared to only relying on the tunable absorption of the graphene. This mechanism enables the design of electro-absorption modulators with significantly reduced size and intrinsic capacitance, critical for integrated photonic circuits with high-speed operation and low power consumption.

References

1. K. S. Novoselov, A. K. Geim, S. Morozov, D. Jiang, Y. Zhang, S. Dubonos, I. Grigorieva, and A. Firsov, Science **306**, 666 (2004).
2. Y.-M. Lin, C. Dimitrakopoulos, K. A. Jenkins, D. B. Farmer, H.-Y. Chiu, A. Grill, and P. Avouris, Science **327**, 662 (2010).
3. L. Britnell, R. V. Gorbachev, R. Jalil, B. D. Belle, F. Schedin, M. I. Katsnelson, L. Eaves, S. V. Morozov, N. M. R. Peres, J. Leist, A. K. Geim, K. S. Novoselov, and L. A. Ponomarenko, Science **335**, 947 (2012).
4. X. Gan, R.-J. Shiue, Y. Gao, I. Meric, T. F. Heinz, K. Shepard, J. Hone, S. Assefa, and D. Englund, Nat. Photonics **7**, 883 (2013).
5. A. Pospischil, M. Humer, M. M. Furchi, D. Bachmann, R. Guider, T. Fromherz, and T. Mueller, Nat. Photonics **7**, 892 (2013).
6. M. Liu, X. Yin, E. Ulin-Avila, B. Geng, T. Zentgraf, L. Ju, F. Wang, and X. Zhang, Nature **474**, 64 (2011).
7. M. Liu, X. Yin, and X. Zhang, Nano Lett. **12**, 1482 (2012).
8. A. Grigorenko, M. Polini, and K. Novoselov, Nat. Photonics **6**, 749 (2012).
9. S. Thongrattanasiri, F. H. L. Koppens, and F. Javier García de Abajo, Phys. Rev. Lett. **108**, 047401 (2012).
10. Y. Fan, Z. Wei, Z. Zhang, and H. Li, Opt Lett. **38**, 5410 (2013).
11. Y. Fan, N.-H. Shen, T. Koschny, and C. M. Soukoulis, ACS Photonics **2**, 151 (2015).
12. G. W. Hanson, J. Appl. Phys. **103**, 064302 (2008).
13. A. B. Kuzmenko, E. van Heumen, F. Carbone, and D. van der Marel, Phys. Rev. Lett. **100**, 117401 (2008).
14. G. Xu, J. Liu, Q. Wang, R. Hui, Z. Chen, V. A. Maroni, and J. Wu, Adv. Mater. **24**, 71 (2012).
15. W. L. Barnes, A. Dereux, and T. W. Ebbesen, Nature **424**, 824 (2003).
16. R. Lu, A. Konzelmann, F. Xu, J. Liu, Q. Liu, M. Xin, R. Hui, and J. Z. Wu, Carbon **86**, 78 (2015).
17. G. V. Naik, J. Kim, and A. Boltasseva, Opt. Mater. Express **1**, 1090 (2011).
18. R. G. Gordon, MRS Bulletin **25**, 52 (2000).
19. L. Liao and X. Duan, Mater. Sci. Eng. R **70**, 354 (2010).
20. S. Kim, J. Nah, I. Jo, D. Shahrjerdi, L. Colombo, Z. Yao, E. Tutuc, and S. K. Banerjee, Appl. Phys. Lett. **94**, 062107 (2009).